كلية الهندسة بشبرا
FACULTY OF ENGINEERING AT SHOUBRA
ERJ
PRINT ISSN 3009-6049
ONLINE ISSN 3009-6022

ENGINEERING RESEARCH JOURNAL (ERJ)
Volume (52),Issue (4)
October 2023, pp:93-98
https://erjsh.journals.ekb.eg

The effect of printing parameters on crushing behavior of 3D printed Poly Lactic Acid/Carbon Fiber samples using Material Extrusion technique

Mina Adel Hanna [1, *], Sameh Shawky Habib [2], Khaled Abdelghany [3], Tamer Samir Mahmoud [2]

[1, *] *Production Engineering and Manufacturing Technology Department, Modern Academy for Engineering and Technology in Maadi, Cairo, Egypt*
[2] *Department of Mechanical Engineering, Faculty of Engineering at Shoubra, Benha University, Cairo, Egypt. Sameh.abadir@feng.bu.edu.eg.*
[3] *Advanced Manufacturing department at The Central Metallurgical Research and Development Institute (CMRDI) - Ministry of Scientific Research, Egypt, Cairo, Egypt. kghany@rpcmrdi.org.*
**Corresponding author*

E-mail address: eng.minaadel17@gmail.com, sameh.abadir@feng.bu.edu.eg, kghany@rpcmrdi.org, tamer.abdelmagid@feng.bu.edu.eg

Abstract: 3D printing products have poor mechanical properties and thus less reliability for longer. Fused deposition modelling (FDM) is commonly used additive manufacturing technology. Mechanical and physical characteristics could be enhanced by checking out several FDM parameters as well as using brand new substances over this technology. This study analyzed the impact and compression strengths of Poly Lactic Acid/Carbon Fiber composites (CF/PLA). The research considered important methodological aspects: the effects of layer patterns (triangular and rectilinear), wall thickness and infilled density on compression and impact mechanical properties of 3D-printed PLA carbon-fibre samples, using an FDM 3D printing machine. The results showed that triangle samples have more mechanical stability and do not collapse suddenly, compared to rectilinear samples. This collapse was observed in the rectilinear samples with 1.2 mm of outer wall thickness and 70% or 85% of infill percentages, while the rectilinear samples showed the highest mechanical performance. The infill density is the most important parameter for all rectilinear samples, as the lowest impact strength of 0.20 kJ/m2 was recorded for a sample with 70% infill and 6 mm wall thickness.

Keywords: Fused deposition modeling, polylactic acid, Short Carbon fiber, Compression, Impact.

1. Introduction

Nowadays, the Present world is observing rapid uptake and great technological maturity in Additive Manufacturing (AM) field. Initially, 3D printing technology emerged mainly for the purpose of fabricating prototypes for functional and visual testing. However, recent applications of 3D printing technology are seen in components of the actual devices or medical appliances [1]. In general, AM reduces the manufacturing overall time and eliminates the necessity for tooling. The manufacturing concept of AM differs from the traditional manufacturing technique. AM is not a formative or subtractive technology, but rather the “final product” is built by adding substance in layers form until produces a finished product [3].

Compared to other AM technologies that are commercially available, FDM is the most prevalent and cost-effective method to print 3D parts [4]. FDM has been applied and enhanced quickly in various fields from automotive, aircraft, electronics to biomedical [5].

Thermoplastic polymers are frequently utilized in the FDM process. The thermos-plasticity of those polymer materials (used as filament) is considered more significant since it enables the filament to melt throughout the printing process and then solidify relatively rapidly at room temperature after deposition. in the group of thermoplastic materials, polylactic acid (PLA) is the most usually used for FDM technology [6]. However, PLA is still not sufficiently good in all applications [7].

For fabricating functional products in addition to prototypes, it is essential to improve a number of properties to fully engage FDM as a manufacturing tool. The functional products require FDM process enhancements for greater control of dimensional and better tolerances, suitable surface finish and enhance mechanical properties of parts to preserve their integrity over the working [8, 9]. A substantial amount of research has been done recently, to evolve the promising technology of FDM. Studies have emphasized the importance of optimizing processing parameters to improve the mechanical properties of the final product.

In this respect, the prototyping tool has been adopted widely in the fabrication of engineering parts, for the FDM process to count as a manufacturing tool. So, it is necessary, its process and material characteristics, such as surface finish and accuracy, tolerance, and uniform material property, need to obtain a high standard of maturity [10]. Moreover, [11] confirmed that FDM 3D printed samples have poorer mechanical properties. Therefore, it is crucial to improve the mechanical properties of FDM 3D printed technology.

Because of the raster-by-raster melting and accumulating formation characteristics of FDM technology, several pores are formed in the sample, lack of strength, stair-step effect (poor surface finish), higher building time, and the deposited Materials rasters are not entirely integrated into one [12].

[13]. They analyzed the effect of printing temperature and printing speed on tensile strength and elastic modulus of PLA parts, increasing of printing temperature increase the tensile strength and elastic modulus firstly and then decrease. The flexural strength increases by decreasing both infill width and layer thickness. Flexural strength is affected by the resistance moment. The smaller the infill width and layer thickness, the smaller amount of gap produced during the 3D printed process as stated by [14].

[15] studied the impact of different lengths and contents of carbon fiber as a reinforcement for thermoplastic matrix CFRP composites on the mechanical properties of FDM-printed parts. Carbon fiber reinforced FDM products showed enhanced mechanical behaviors for the parts, and this was proved by watching the fracture interface with an SEM micrograph. FDM feedstock filaments were fabricated with three different contents of fiberglass reinforcement in an ABS matrix to examine the improvement in mechanical properties. The results showed that fiberglass significantly enhanced the surface rigidity and tensile strength of the ABS filament.

This research examines the crushing behavior under compression and impact for triangular and rectilinear structure samples made of short-fiber-reinforced Polylactic Acid printed by the FDM process. The study compares printing parameters and investigates the impact of different building patterns, infill percentages, and wall thicknesses on the mechanical characteristics of PLA/CF samples.

2. Experimental procedure

2.1 Materials

In this research, Carbon Fiber Polylactic Acid (PLA/CF) Filament of diameter 1.75 mm (supplied by ISANMATE, China) used as feedstock. Carbon Fiber Polylactic Acid Filament consists of 80% nylon and 20% chopped carbon fiber. The mechanical characteristics of used (PLA/CF) Filament as attached in the supplier company data sheet are summarized in Table1.

2.2 Specimen design and the 3D printing process

The CREALITY Ender-3 3D printer, manufactured by CREALITY-3D Printing in China, was used to fabricate PLA/CF samples from the original shape as filament using Fused Deposition Modeling (FDM) technology. The printing parameters were adjusted and the necessary G-Code for the FDM process was generated using Ultimaker Cura 4.3 software. According to the material supplier recommendation, the fixed FDM printing parameters for PLA/CF are listed in Table 2.

To study the mechanical properties of printed samples, 2D rectilinear and triangle structures were chosen based on previous research. These structures allow for a comprehensive assessment of how the material properties and geometrical features affect mechanical behaviors. The specimens were designed using SolidWorks 2018 software. Each specimen had different parameters such as wall thickness, infill pattern and infill percentage, as shown in Fig.1. The specimens had one open square face and one closed square face. The printing direction was along the Z axis, with the closed square face on the printer bed. The specimens followed ASTM standards for mechanical experiments. The slicer software generated G-code from the STL Files of the samples and transferred it to the 3D printing machine.

Table 1 mechanical properties of PLA-CF filament.

PLA-CF filament			
Mechanical properties	Value	Unit	Test Standard
Tensile Strength, Break	48	MPa	ISO 527
Tensile Modulus	4950	MPa	ISO 527
Tensile Elongation, Break	2	%	ISO 527
Flexural Strength	89	MPa	ISO 178
Flexural Modulus	6320	MPa	ISO 178

Table 2 constant parameters during FDM printing process PLA-CF.

PLA/CF	
Nozzle Diameter	0.4 mm
Layer Height	0.12 mm
Printing Speed	45 mm/min
Reaction Speed	35 mm/min
Nozzle Temperature	190◦C
Bed Temperature	60◦C
Fill Angles	45◦, -45◦

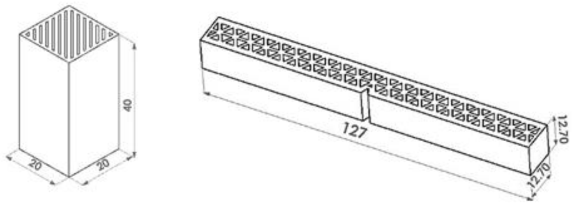

(a) **(b)**

Fig. 1. (a) Specimen for compression testing, **(b)** Specimen for impact testing, with infill density 70%, and 1.2-mm wall- thickness.

The experiment used a Central Composite-Face-centered Design (CCF) for three parameters: wall thickness, infill percentage, and infill pattern. Three levels were considered for wall thickness and infill percentage for both triangle and rectilinear patterns. CCF is efficient and practical. A total of 28 experiments were conducted, including nine for each pattern and five replicates at the central point for each pattern.

2.3 Compressive tests

According to ASTM D695, compression test samples must be cylindrical or prismatic with a diameter/side to length ratio of 1 to 2. A cube shape with dimensions of 20x20x40 mm was chosen for this research. Compression tests were conducted at the National Institute for Standards (NIS) on a universal testing machine (UTM) with a 100 kN load cell per ASTM D695. Tests ended at fracture or 50% strain. Energy Absorption (EA) was calculated from the area under the stress-strain curve (Equation (2)):

$$\text{EA} = \int_a^b \sigma . d\varepsilon \qquad (1)$$

Where σ is the compressive stress and the ε denotes the nominal strain. The SEA is obtained using EA and specimen weight.

$$\text{SEA} = \frac{EA}{m} \qquad (2)$$

The mean crushing force (MCF) and crushing force efficiency (CFE) were calculated as follows:

$$\text{MCF} = \frac{1}{\delta_d} \int_0^{\delta_d} F\delta_d \qquad (3)$$

$$\text{CFE} = \frac{MCF}{IPF} \qquad (4)$$

Where F and δ are the compressive force and displacement and IPF is initial peak force

2.4 Impact tests

Charpy impact tests were conducted on a Zwick/Roell HIT (Zwick/Roell GmbH, Ulm, Germany) pendulum impact tester per DIN EN ISO 179-1:2010 for standard notched specimens. Samples were designed as the maximum recommended notch dimensions of 12.7x12.7x127 mm per ASTM D6110 [52]. Energy lost through sample fracture is proportional to the difference in pendulum height before and after impact.

3. Results and discussion

3.1 Compression properties

Experiments showed that 3D-printed triangle infill pattern PLA/CF filament materials with varying wall thickness (1.2, 3.6, 6 mm) and infill percentage (70, 85, 100%) displayed slightly different distortion patterns and mechanical characteristics under compression testing.

3.1.1 Triangular pattern samples

Figure 2 shows the stress-strain curve of printed PLA/CF. Equivalent compression stress is calculated as $\sigma = F/A$. Crushing behavior of 3D fabricated specimens during compression can be classified as stable (gradually) or unstable (sudden). Stress-Strain Response of triangle-patterned samples is a stable (progressive) crashing. The curves present similar evolutionary styles, that are divided into three stages: (i) start by a linear elastic deformation zone; (ii) until initial peak force (a stress plateau); with the stress fluctuations, the first collapses are developed at critical nodes (stress concentration points), which is a thickness variations or corners; the collapsing mode is maintained, and stress levels fall significantly as a result of cell walls buckling and forming a significant geometrical change at critical nodes. (iii) at the last stage, a gradual strain hardening developed because of the contact of inner cellular structure walls.

PLA/CF samples have fewer stress fluctuations and a slight drop in load during crushing. Early collapsing at the junction of angled and vertical walls may caused rapid folding of the sample structure. The significant decrease in stress is due to strain localization and increased porosity of the inter-bead in the PLA/CF structure.

The modulus of elasticity of PLA/CF samples is small for all triangle pattern samples based on the results presented in Fig. 3a. The inclusion of carbon fibers has a negative impact on compressive strength due to their orientation in the printing plane (x-y plane), which is parallel to the printing direction. The carbon fibers in the sample walls are not exposed to their stronger stretching deformation mode under compression stress as the short fibres in the x-y plane at any z-level are orthogonal to the direction of compression.

SEA is important in assessing the compression resistance of 3D-printed lightweight products. As shown in Fig. 3b, the addition of CF to PLA results in an unstable SEA trend for the triangular pattern due to a decrease in the ductility of the PLA material, reducing its ability to absorb energy through plastic deformation.

CFE measures the consistency and stability of force during collapse under loading (Fig. 3c). The addition of CF to PA results in an unclear and unstable trend for the CFE of the triangular pattern across all samples. The sample with a wall thickness of 6mm and an infill percentage of 85% has the highest CEF value (0.915), while the sample with a wall thickness of 1.2mm and an infill percentage of 85% has the lowest CEF value.

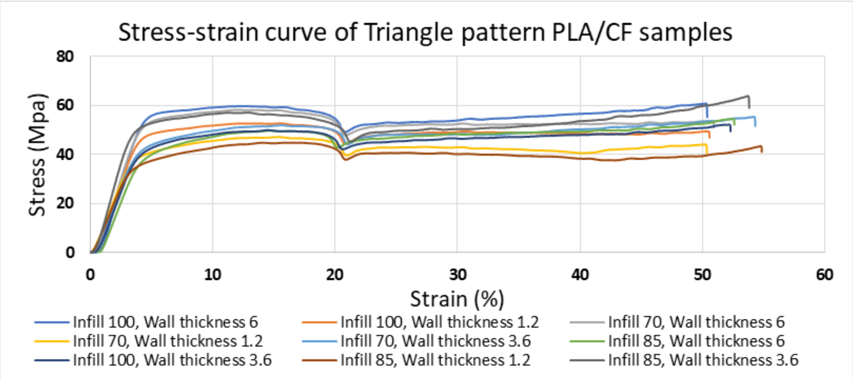

Fig. 2. Compression behavior of the 3D printed samples: Characteristic compression stress-strain curves of Triangle pattern for PLA/CF.

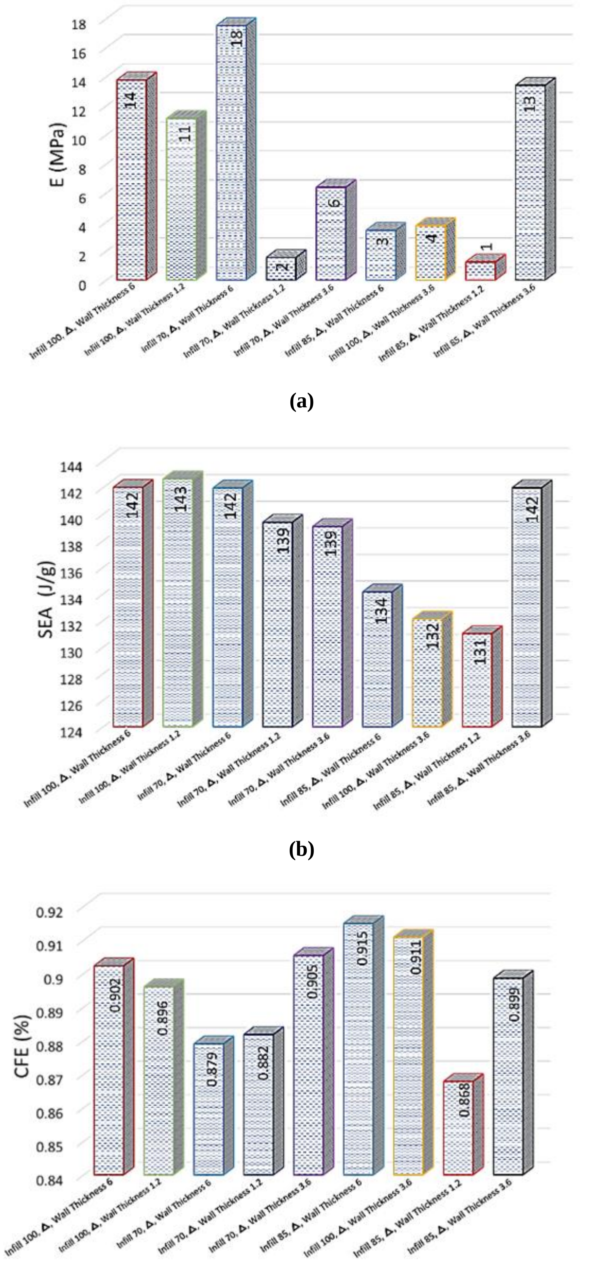

(a)

(b)

(c)

Fig. 3. Graphical comparison of triangular CF/PLA samples under compression: (a) modulus of elasticity (E), (b) specific energy absorption (SEA), and (c) crushing force efficiency (CFE).

3.1.2 Rectilinear pattern samples

Figure 4 shows the nominal stress-strain of rectilinear PLA/CF structure under compression load. The compressive behavior of the rectilinear pattern is independent of infill percentage for the same base material and relative density. After an initial linear elastic region, all samples display a well-defined yield point, followed by a significant drop in stress due to wall buckling. Samples with an outer wall thickness of 1.2 mm and infill percentages of 70% and 85% exhibit catastrophic collapse behavior.

Figure 5 shows the crashworthiness factors (E, SEA, CFE) from the stress-strain responses. The triangle pattern crushed more stable than the rectilinear pattern. For PLA/CF samples, the lowest E values (3.20 and 5.98 MPa) were for 70% and 85% infill and 3.6 mm and 1.2 mm wall thicknesses. The lowest SEA (20 J/g) and CFE (0.65%) were for 85% infill and 1.2 mm wall thickness. Wall thickness affected compression strength more than infill percentage.

The Es, SEAs, and CFEs of PLA/CF rectilinear samples do not exhibit a stable trend, due to the random distribution of short carbon fibers and their orientation. The high inter-bead porosity due to the unsteady flow of PLA/CF melt during printing, reducing their stiffness. High porosity in PLA/CF may also be responsible for irregularities in the stress-strain results.

3.1.3 Effect of Outer Wall Thickness on Compression Strength.

Figures 6 shows that compressive strength is positively affected by outer wall thickness. At 70% infill percentage, an improvement of 24% for PLA/CF was seen for the triangle pattern from 1.2 mm to 6 mm outer wall thickness. For the rectilinear pattern at 70% infill percentage, an increase in compression strength of 68% (PLA/CF) was seen from 1.2 mm to 6 mm outer wall thickness. This may be due to the increased rigidity of samples with increased envelope wall thickness.

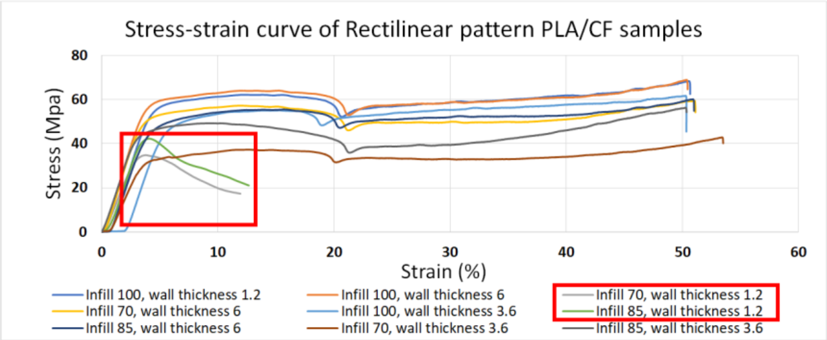

Fig. 4. Compression behavior of the 3D printed samples: Characteristic compression stress-strain curves of Rectilinear pattern for CF/PLA.

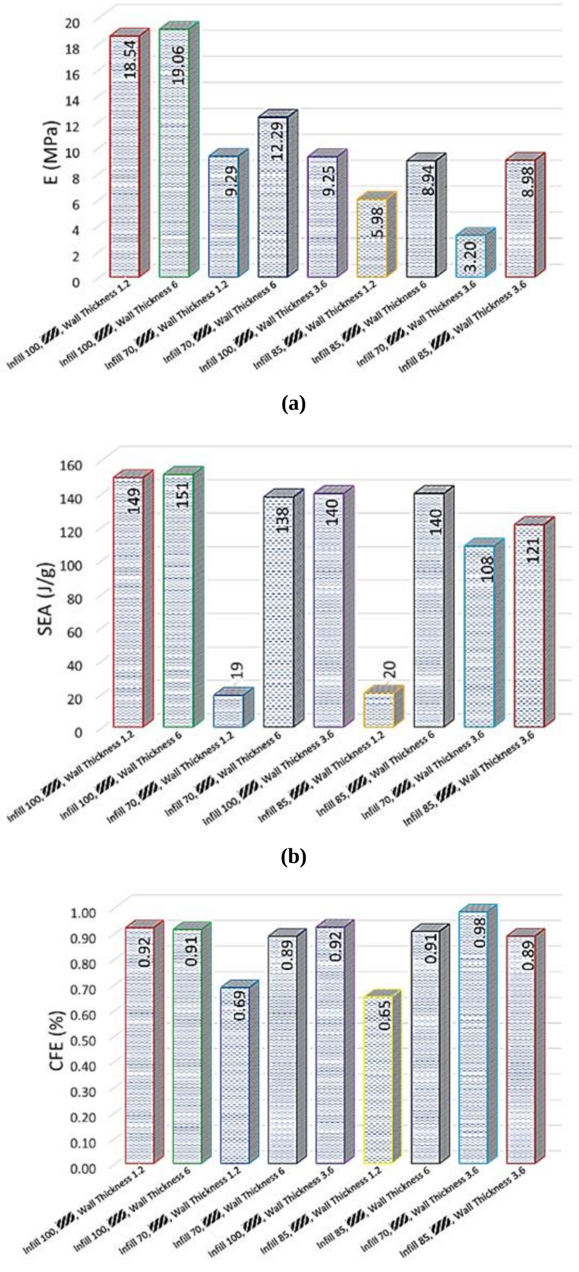

(a)

(b)

(c)

Fig. 5. Graphical comparison of Rectilinear CF/PLA samples under compression: (a) modulus of elasticity (E), (b) specific energy absorption (SEA), and (c) crushing force efficiency (CFE).

3.1.4 Effect of Infill Percentage on Tensile Strength.

Figures 6 show that compression strength increases with an increase in infill percentage. At a wall thickness of 1.2 mm, a maximum increase of 82% (PLA/CF- Rectilinear pattern) and 11% (PLA/CF- Triangle pattern) in compression strength was observed from 70% to 100% infill percentage. The triangular pattern samples showed a smaller increasing trend of compression strength compared to rectilinear pattern samples for PLA/CF.

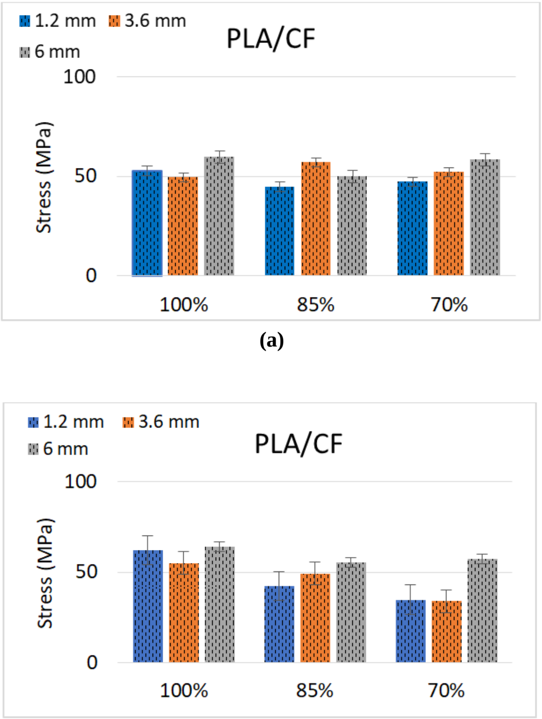

(a)

(b)

Fig. 6. Comparison of the compression stress results of **(a)** triangular and **(b)** rectilinear pattern samples.

3.2 Impact strength

3.2.1 Triangular pattern samples

Figure 7 provides a diagrammatic representation of the test results. The impact results of the triangle pattern PLA/CF material are shown in Fig.7a. Samples with a high infill percentage have better impact strength characteristics, while wall thickness has a negligible effect. The PLA/CF sample with the highest infill percentage (100%) and medium wall thickness (3.6 mm) had high impact resistance of 1.7 kJ/m^2.

3.2.2 Rectilinear pattern samples

Figure 7b presents the impact strength of rectilinear pattern PLA/CF specimens decreased slightly. The highest strength of 1.96 kJ/m2 was achieved by a specimen with 85% infill and 3.6 mm wall thickness, while the lowest strength of 0.20 kJ/m^2 was observed for a specimen with 70% infill and 6 mm wall thickness. Wall thickness did not have a significant effect on Charpy impact strength. A slightly higher strength was seen for specimens with a high infill percentage. Chopped carbon fiber adversely affected Charpy impact strength.

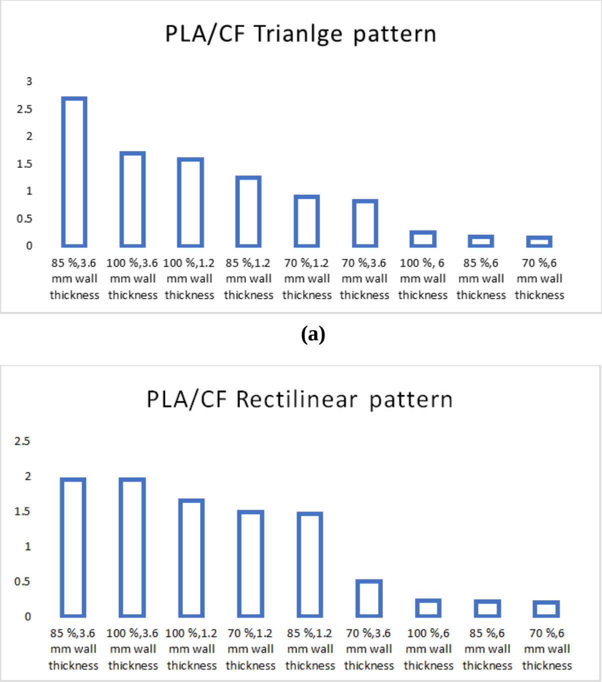

(a)

(b)

Fig. 7 Impact strength results of **(a)** triangular and **(b)** rectilinear pattern samples.

4. Conclusions

This study examined the effect of wall thickness and infill percentage on the compression and impact strength of PLA/CF 3D-printed samples with triangular and rectilinear patterns. The results showed that infill percentage had a major impact on both compression and impact strength for both patterns, while wall thickness had a minor impact. The rectilinear sample with 6 mm wall thickness and 100% infill achieved the highest compression strength (36 MPa), while the rectilinear sample with 3.6 mm wall thickness and 85% infill achieved the highest impact strength (1.96 kJ/m^2). The triangular sample with 1.2 mm wall thickness and 70% infill had the lowest compression strength (7 MPa), while the rectilinear sample with 6 mm wall thickness and 70% infill had the lowest impact strength (0.20 kJ/m^2). These findings indicate that infill percentage is a crucial parameter for enhancing the mechanical performance of 3D-printed PLA/CF structures.

5. References

[1] Kim H, Park E, Kim S, Park B, Kim N, Lee S: Experimental Study on Mechanical Properties of Single- and Dual-material 3D Printed Products. Procedia Manufacturing 2017, 10:887-897.

[2] Wohlers TJWA, Fort Collins, CO: Additive manufacturing and 3D printing state of the industry. 2013, 6:269-375.

[3] Maidin S, Muhamad M, Pei E: Feasibility study of ultrasonic frequency application on fdm to improve parts surface finish. 2015.

[4] Yadav P, Sahai A, Sharma RS: Strength and Surface Characteristics of FDM-Based 3D Printed PLA Parts for Multiple Infill Design Patterns. Journal of The Institution of Engineers (India): Series C 2020, 102(1):197-207.

[5] Prayitno G, Imaduddin F, Ubaidillah, Arifin Z: Recent Progress of Fused Deposition Modeling (FDM) 3D Printing: Constructions, Parameters and Processings. IOP Conference Series: Materials Science and Engineering 2021, 1096(1).

[6] Akhoundi B, Nabipour M, Hajami F, Shakoori D: An Experimental Study of Nozzle Temperature and Heat Treatment (Annealing) Effects on Mechanical Properties of High-Temperature Polylactic Acid in Fused Deposition Modeling. Polymer Engineering & Science 2020, 60(5):979-987.

[7] Ngo TD, Kashani A, Imbalzano G, Nguyen KTQ, Hui D: Additive manufacturing (3D printing): A review of materials, methods, applications and challenges. Composites Part B: Engineering 2018, 143:172-196.

[8] Popescu D, Zapciu A, Amza C, Baciu F, Marinescu R: FDM process parameters influence over the mechanical properties of polymer specimens: A review. Polymer Testing 2018, 69:157-166.

[9] Bayraktar Ö, Uzun G, Çakiroğlu R, Guldas A: Experimental study on the 3D-printed plastic parts and predicting the mechanical properties using artificial neural networks. Polymers for Advanced Technologies 2017, 28(8):1044-1051.

[10] Tofangchi A, Han P, Izquierdo J, Iyengar A, Hsu K: Effect of Ultrasonic Vibration on Interlayer Adhesion in Fused Filament Fabrication 3D Printed ABS. Polymers (Basel) 2019, 11(2).

[11] Wu W, Geng P, Li G, Zhao D, Zhang H, Zhao J: Influence of Layer Thickness and Raster Angle on the Mechanical Properties of 3D-Printed PEEK and a Comparative Mechanical Study between PEEK and ABS. Materials (Basel) 2015, 8(9):5834-5846.

[12] Torrado AR, Roberson DA: Failure Analysis and Anisotropy Evaluation of 3D-Printed Tensile Test Specimens of Different Geometries and Print Raster Patterns. Journal of Failure Analysis and Prevention 2016, 16(1):154-164.

[13] Tang C, Liu J, Yang Y, Liu Y, Jiang S, Hao W: Effect of process parameters on mechanical properties of 3D printed PLA lattice structures. Composites Part C: Open Access 2020, 3.

[14] Suteja TJ, Soesanti A: Mechanical Properties of 3D Printed Polylactic Acid Product for Various Infill Design Parameters: A Review. Journal of Physics: Conference Series 2020, 1569(4).

[15] Ning F, Cong W, Qiu J, Wei J, Wang S: Additive manufacturing of carbon fiber reinforced thermoplastic composites using fused deposition modeling. Composites Part B: Engineering 2015, 80:369-378.D. Bandyopadhyay and J. Sen, “Internet of things: Applications and challenges in technology and standardization,” Wirel. Pers. Commun., vol. 58, no. 1, pp. 49–69, 2011.